Bioactivity of Synthetic 2-Halo-3-aryl-4(3*H*)-quinazoliniminium Halides in L1210 Leukemia and SK-BR-3 Mammary Tumor Cells *In Vitro*

JEAN-PIERRE H. PERCHELLET[1], ANDREW M. WATERS[1], ELISABETH M. PERCHELLET[1], VIJAYA K. NAGANABOINA[2], KUSUM L. CHANDRA[2], JOHN DESPER[2] and SUNDEEP RAYAT[2]

[1]*Anti-Cancer Drug Laboratory, Division of Biology, Ackert Hall, and* [2]*Department of Chemistry, Kansas State University, Manhattan, KS, U.S.A.*

Abstract. *Background: Because quinazolines and their derivatives exhibit a wide range of pharmacological profiles, there is a continuous interest among synthetic and medicinal chemists in the discovery of more potent analogs. Ten novel quinazoliniminium salts were synthesized and tested for their effectiveness against murine and human tumor cell proliferation in vitro. Materials and Methods: Various markers of tumor cell metabolism, DNA degradation and mitotic disruption were assayed in vitro to evaluate drug cytotoxicity. Results: All compounds induced concentration- and time-dependent antitumor effects in vitro but the 2-chloro-3-(4-methoxyphenyl)quinazolin-4(3H)-iminium chloride (**4**) was the most effective inhibitor of leukemia L1210 cell proliferation at days 2-4 (IC_{50}: 2.1-0.9 μM), suggesting that the para-methoxyphenyl substituent on the N3 of **4** may enhance the antiproliferative properties of the quinazoliniminium scaffold. In mammary SK-BR-3 tumor cells, **4** reduced the Ki-67 marker of cell proliferation at 24 h and the metabolic activity at days 2 and 4. Moreover, a 1.5- or 3-h treatment with **4** was sufficient to inhibit the rates of DNA, RNA and protein syntheses measured in L1210 cells over 0.5- or 1-h periods of pulse-labeling with ^{3}H-thymidine, 3H-uridine and ^{3}H-leucine, respectively. As **4** did not reduce the fluorescence of the ethidium bromide-DNA complex, this compound was unlikely to directly bind to or destabilize double-stranded DNA. However, **4** induced DNA cleavage at 24 h in L1210 cells containing ^{3}H-thymidine-prelabeled DNA, suggesting that this antitumor drug might trigger an apoptotic pathway of DNA fragmentation. After 12-48 h, **4** weakly increased the mitotic index of L1210 cells but stimulated the formation of many binucleated cells, multinucleated cells and micronuclei, suggesting that this antitumor compound might enhance mitotic abnormality, induce chromosomal damage or missegregation, and block cytokinesis. Conclusion: Although **4** may have interesting bioactivity, more compounds based on the quinazoliniminium scaffold must be synthesized to elucidate structure–activity relationships, identify more potent antitumor lead compounds, and investigate their molecular targets and mechanisms of action.*

Correspondence to: J.-P. Perchellet, Anti-Cancer Drug Laboratory, Kansas State University, Division of Biology, Ackert Hall, Manhattan, KS 66506-4901, U.S.A. Tel: +1 7855327727, Fax: +17855326653, e-mail: jpperch@ksu.edu

Key Words: Quinazoliniminium salts, tumor cell proliferation, Ki-67 expression, macromolecule syntheses, DNA interaction and fragmentation, multiple mitotic figures, nuclei, micronuclei.

Quinazolinones and their derivatives are regarded as 'privileged structures' capable of binding to multiple receptors with high affinity (1) and exhibit a broad spectrum of antihypertensive (2-4), antimalarial (5), antimicrobial (6-8), antiobesity (9), anticonvulsive (10), anticancer (11), anti-inflammatory (12, 13) and analgesic (14, 15) bioactivities. These heterocycles have also found applications as organic dyes (16, 17) and fluorescent chemosensors for the detection of heavy metals (18). The 4(3*H*)-quinazolinimine scaffold is an important building block for the synthesis of quinazolinones and their derivatives, and various quinazolinimines have also been reported to inhibit acetylcholinesterase (19) and butyrylcholinesterase (20-22) activities. However, the antiproliferative activities of quinazolinimines have not been explored. The presence of this core structure may afford heterocyclic compounds with increased activity, lower toxicity and better pharmacological profiles than the currently known derivatives of quinazolines. Hence, novel 2-halo-3-aryl-4(3*H*)-quinazoliniminium halides were synthesized and evaluated for their antiproliferative activity in rapidly growing suspension cultures of L1210 leukemia cells and slow-growing monolayer cultures of SK-BR-3 mammary tumor cells, using tests of metabolic activity, macromolecule syntheses, DNA fragmentation and mitotic

disruption *in vitro* (23). Since the fraction of Ki-67-positive tumor cells is often correlated with the clinical course of cancer, it was also of interest to determine whether quinazoliniminium salts would inhibit the expression of human Ki-67 nuclear protein, which is an excellent marker of tumor cell proliferation (24).

Materials and Methods

Drug treatment, cell culture and proliferation assay. An efficient three-step synthesis of 2-halo-3-aryl-4(3*H*)-quinazoliniminium halides has been developed and will be reported elsewhere. Ten novel quinazoliniminium salts were synthesized, using aza-Wittig reaction of aminobenzonitrile to produce iminophosphorane, which upon treatment with phenyl isocyanates yielded benzannulated cyano-ene-carbodiimides. The latter underwent facile intramolecular cyclization to 2-halo-3-aryl-4(3*H*)-quinazoliniminium halides upon treatment with hydrogen halides generated *in situ*. Solutions of synthetic quinazoliniminium salts and known anticancer drugs used as positive controls (all from Sigma-Aldrich, St. Louis, MO, USA) were dissolved and serially diluted in dimethyl sulfoxide (DMSO). Suspension cultures of murine L1210 lymphocytic leukemia cells and monolayer cultures of human SK-BR-3 breast adenocarcinoma cells (both from ATCC, Manassas, VA, USA) were incubated at 37˚C in a humidified atmosphere containing 5% CO_2 and maintained in continuous exponential growth by twice-a-week passage in RPMI-1640 medium supplemented with 10% fetal calf serum (FCS; Atlanta Biologicals, Norcross, GA, USA) and penicillin (100 IU/ml)-streptomycin (100 μg/ml). L1210 cell suspensions were grown in triplicate in 48-well Costar cell culture plates for 2 and 4 days in the presence or absence (control) of serial concentrations of synthetic quinazoliniminium salts to evaluate their antiproliferative activity. Adherent SK-BR-3 cells were collected by trypsinization, resuspended in fresh FCS-containing RPMI-1640 medium, plated in 48-well Costar cell culture plates, and allowed to attach for 24 h before being incubated for an additional 2-4 days in the presence or absence (control) of the above drugs. Since compounds were supplemented to the culture medium in 1-μl aliquots, the concentrations of vehicle in the final incubation volume (0.5 ml) never exceeded 0.2% and did not interfere with the data. Decreasing concentrations of cells, such as 45,000 and 2,500 L1210 cells/0.5 ml/well or 15,000 and 5,000 SK-BR-3 cells/0.5 ml/well were initially plated in triplicate at time 0 in order to collect control samples with approximately equal cell densities after 2 and 4 days in culture, respectively (23). The proliferation of control and drug-treated tumor cells was assessed from their mitochondrial ability to bioreduce the 3-(4,5-dimethylthiazol-2-yl)-5-(3-carboxymethoxyphenyl)-2-(4-sulfophenyl)-2*H*-tetrazolium (MTS) reagent (Promega, Madison, WI, USA) in the presence of phenazine methosulfate (PMS; Sigma) into a water-soluble formazan product that absorbs at 490 nm (25). After 2 or 4 days in culture, control and drug-treated L1210 or SK-BR-3 cell samples were further incubated at 37˚C for 2 h in the dark in the presence of 0.1 ml of MTS:PMS (2:0.1) reagent and their relative metabolic activity was estimated by recording the absorbance at 490 nm, using a Cambridge model 750 automatic microplate reader (Packard, Downers Grove, IL, USA) (23). Blank values for culture medium supplemented with MTS:PMS reagent in the absence of cells were subtracted from the results. Data of all biochemical experiments were analyzed using Student's *t*-test with the level of significance set at $p<0.05$.

Whole cell immunodetection of Ki-67 protein level. For Ki-67 expression, SK-BR-3 cells (5×10^3 cells/0.2 ml) were seeded into 96-well Nunc F96 MicroWell polystyrene white plates (Thermo Fisher Scientific, Waltham, MA, USA), allowed to attach for 24 h at 37˚C, and then incubated for an additional period of 24 h in the presence or absence (control) of drugs. After removing the culture medium by suction, the adherent cells in each well were washed twice with 100 μl of Ca^{2+}/Mg^{2+}-free Dulbecco's phosphate-buffered saline (PBS) and fixed for 10 min in 100 μl of ice-cold MeOH. The MeOH was removed by washing with PBS (2×100 μl) and the cells were lysed in 100 μl of PBS, containing 0.1% Triton X-100, for 15 min at room temperature. After washing with 20 mM Tris-HCl buffer, pH 7.4, containing 0.9% of NaCl and 0.05% of Tween-20 (TBST) (2×100 μl), the plates were further incubated with 100 μl of SuperBlock (Pierce, Rockford, IL, USA) for 1 h at room temperature. After aspirating the SuperBlock, the plates were then incubated overnight at 4˚C with rabbit anti-Ki-67 (H-300) primary polyclonal antibody (Santa Cruz Biotechnology, Santa Cruz, CA, USA) at a 1:100 dilution in SuperBlock (50 μl/well). Each well was washed with TBST (2×100 μl) and incubated for 1 h at room temperature with both horseradish peroxidase-linked anti-rabbit IgG secondary monoclonal antibody (1:500 dilution; Oncogene, Boston, MA, USA) and Hoechst 33342 reagent (1:5,000 dilution; Invitrogen, Molecular Probes, Eugene, OR, USA) in 50 μl of SuperBlock. After washing with TBST (2×100 μl) to remove the unbound antibody and adding the SuperSignal West Pico Chemiluminescence (CL) Substrate (50 μl/well), plates were read within 5 min by scanning each well for 0.1 s in the CL mode (425 nm) of a Cary Eclipse Fluorescence Spectrophotometer equipped with a microplate reader (Varian, Walnut Creek, CA, USA). Readings from wells where the primary polyclonal antibody was omitted were used to subtract the background CL. Finally, the plates were read in the fluorescence mode (340 nm excitation/461 nm emission) of the same Cary Eclipse fluorescence microplate reader. The relative fluorescence intensities of the Hoechst reagent–DNA complexes were used to normalize the relative CL unit values of the primary antibody-antigen immune complexes bound to the horseradish peroxidase-linked secondary antibody in order to compare Ki-67 protein levels on an equal cell number basis. The ratio of relative luminescence:fluorescence was expressed as % of that for vehicle-treated control cells.

Macromolecule syntheses. To estimate the rate of DNA synthesis, L1210 cells were resuspended in fresh FCS-containing RPMI–1640 medium at a density of 0.5×10^5 cells/0.5 ml, incubated at 37˚C for 90 min in the presence or absence (control) of drugs and then pulse-labeled for an additional 30 min with 1 μCi of [methyl-^{3}H]thymidine (52 Ci/mmol; GE Healthcare-Amersham, Piscataway, NJ, USA) (23). For RNA and protein syntheses, cells were incubated at 37˚C for 3 h in the presence or absence of drugs and then pulse-labeled for an additional 1 h with 2 μCi of [5,6-^{3}H]uridine (35 Ci/mmol; PerkinElmer, Boston, MA, USA) or 2.5 μCi of L-[3,4,5-^{3}H]leucine (115 Ci/mmol; PerkinElmer), respectively (23). The incubations were terminated by the addition of 2 ml of 10% trichloroacetic acid (TCA). After holding on ice for 15 min, the acid-insoluble material was recovered over Whatman GF/A glass microfiber filters and washed thrice with 2 ml of 5% TCA and twice with 2 ml of 100% EtOH. After drying the filters, the radioactivity bound to the acid-precipitable material was determined by liquid scintillation counting (LSC) in 6 ml of Bio-Safe NA (Research Products International, Mount Prospect, IL, USA) (23).

DNA binding and fragmentation assays. An ethidium bromide (EB) displacement assay was used to assess the eventual DNA-binding potencies of quinazoliniminium salts, based on the IC_{50} concentrations of drugs that cause a 50% reduction in the fluorescence of the DNA-EB complex at 525 nm excitation/600 nm emission (26). The fluorescence of EB, which is extremely low when unbound in water, is boosted 25-fold after binding and intercalating in the hydrophobic environment of the intact double-stranded DNA. Since a highly fluorescent complex is formed within milliseconds between DNA and EB, any drug directly binding to and/or damaging DNA would disrupt EB intercalation and compromise the fluorescence of this EB-DNA complex. The reaction mixtures (200 μl), containing final concentrations of 20 μg/ml calf thymus (ct) DNA (Sigma) and 1 μg/ml EB (Sigma) in 5 mM Tris-HCl buffer, pH 7.6, with 0.5 mM EDTA, were pipetted into 96-well Costar white opaque polystyrene assay plates and, after incubation in the presence or absence (control) of drugs for 30 min at room temperature, the fluorescence of the EB-DNA complex was detected at 525 nm excitation and 600 nm emission, using a Cary Eclipse Fluorescence microplate reader accessory (Varian) (23). Drug-induced DNA cleavage was determined by intact chromatin precipitation, using L1210 cells which were prelabeled with 1 μCi of [^{3}H]thymidine for 2 h at 37˚C, washed with 3×1 ml of ice-cold PBS, collected by centrifugation, resuspended in fresh medium at a density of 1.2×10^6 cells/ml, and then incubated at 37˚C for 24 h in the presence or absence of drugs (23). After centrifugation at 200 ×*g* for 10 min to discard the drugs and wash the cells, the cell pellets were lysed for 20 min in 0.5 ml of ice-cold hypotonic lysis buffer (10 mM Tris-HCl, pH 8.0, 1 mM EDTA and 0.2% Triton X-100), and centrifuged at 12,000 ×*g* for 15 min to collect the supernatants. The radioactivity in the supernatants (detergent-soluble low molecular weight DNA fragments) and the pellets (intact chromatin DNA) was determined by LSC. Before being counted in 6 ml of Bio-Safe NA, the intact pelleted chromatin was incubated for 2 h at 60˚C in the presence of 0.6 ml of NCS tissue solubilizer (Amersham) (23).

Mitotic index and abnormalities. To determine the mitotic index, L1210 cells (0.5×10^6/0.5 ml of FCS-containing RPMI-1640 medium) were incubated in triplicate for various periods of time at 37˚C in the presence or absence (control) of serial concentrations of experimental drugs or known microtubule-disrupting agents, collected by centrifugation (200 ×g × 10 min), and resuspended in 1 ml of hypotonic 75 mM KCl for 20 min at 4˚C. After fixation in 1 ml of MeOH:acetic acid (3:1), the final cell pellets were collected by centrifugation, resuspended in 75 μl of MeOH:acetic acid (3:1), dispensed onto glass slides, air dried, and stained by spreading 40 μl of 0.1% crystal violet under a coverslip (23). Mitotic figures with condensed chromosomes were identified microscopically and published criteria were followed to score binucleated cells, multinucleated cells and micronuclei (27). Cytokinesis-blocked binucleated cells contained either 2 separate nuclei of equal size, 2 nuclei that touched or overlapped with distinct nuclear boundaries, or 2 nuclei that were linked by a small nucleoplasmic bridge (27). Viable cells with 3 (trinucleated) or 4 (quadrinucleated) distinct nuclei were scored as typical multinucleated cells (27). Dot-like chromatin-containing structures in the cytoplasm, at least 1/3 smaller than the main nucleus, surrounded by a membrane either separated from or marginally overlapping the main nucleus, and having the same staining as the main nucleus were scored as micronuclei containing either a whole chromosome or an acentric chromosomal fragment (27). The frequencies of binucleated cells, multinucleated cells and micronuclei were used to estimate the ability of cytotoxic or genotoxic (mutagenic or clastogenic) drugs to block cytokinesis and induce chromosomal damage or missegregation (27). The percentage of cells in mitosis or with 2 nuclei, 3-4 nuclei and micronuclei were determined microscopically by counting a total of at least 2,000 cells/slide and the mitotic, binucleated and multinucleated cell indexes were calculated as percentage of mitotic figures or binucleated and multinucleated cells in drug-treated cultures to that of mitotic figures or binucleated and multinucleated cells in vehicle-treated controls (23, 27).

Results

Inhibition of tumor cell proliferation. The chemical structures and code names of the 10 novel quinazoliniminium halides synthesized and tested for their ability to inhibit tumor cell proliferation *in vitro* are depicted in Figure 1. All compounds tested inhibited, in a concentration-dependent manner, the proliferation of suspension cultures of murine L1210 lymphocytic leukemia cells after 2 and 4 days *in vitro* (Table I). Based on the comparative IC_{50} values required to inhibit the mitochondrial ability of L1210 cells to metabolize the MTS:PMS reagent at days 2 and 4, the 2-chloro-3-(4-methoxyphenyl)quinazolin-4(3*H*)-iminium chloride **4**, which was consistently effective in the low μM range, was selected as the most potent lead antiproliferative compound of the series for further studies (Table I). Indeed, antiproliferative compound **4** retained its ability to inhibit, in the low μM range, the metabolic activity of monolayer cultures of human SK-BR-3 breast adenocarcinoma cells (Table I). Full concentration–response curves indicate that the inhibition of tumor cell growth by the most effective antiproliferative compound **4**, which began around 0.64 μM in L1210 cells and 0.256-1.6 μM in SK-BR-3 cells and became maximal or near maximal around 1.6-10 μM in L1210 cells and 4-25 μM in SK-BR-3 cells, were generally more pronounced after 4 than 2 days in culture (Figure 2). Although the IC_{50} values of **1** and **6** indicate that they are less potent (Table I), these other bioactive compounds also induce concentration-dependent inhibitory effects that, at 10 μM, respectively blocked L1210 tumor cell proliferation at day 4 by 90-100% and, at 25 μM, respectively blocked SK-BR-3 tumor cell proliferation at day 4 by 95-100% (data not shown). However, when tested as positive controls in the same experiments, established anticancer drugs such as daunorubicin (DAU) and mitoxantrone (Mitox) inhibited the growth of L1210 and SK-BR-3 tumor cells at lower nM concentrations (data not shown).

Inhibition of Ki-67 expression. The antitumor activity of **1**, **4** and **6** is substantiated by the finding that these drugs mimic the ability of Mitox to inhibit the expression of the human Ki-67 marker of cell proliferation in SK-BR-3 mammary tumor cells at 24 h (Figure 3). The Ki-67 nuclear protein,

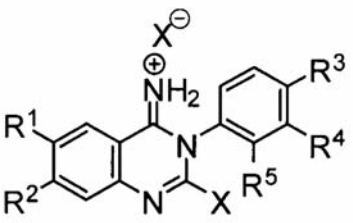

Compounds	X	R^1	R^2	R^3	R^4	R^5
1	Cl	H	H	H	H	H
2	Br	H	H	H	H	H
3	I	H	H	H	H	H
4	Cl	H	H	OMe	H	H
5	Cl	H	H	COOEt	H	H
6	Cl	H	H	Cl	H	H
7	Cl	H	H	H	Cl	H
8	Cl	H	H	H	H	Cl
9	Cl	Me	H	H	H	H
10	Cl	H	Me	H	H	H

Figure 1. *Chemical structures and numbers of the synthetic quinazoliniminium halides tested for their antiproliferative activity in vitro.*

Table I. *Antiproliferative activity of synthetic quinazoliniminium halides in L1210 and SK-BR-3 tumor cells in vitro.*

Compounds	IC_{50} values (μM)[a] in L1210 cells at		IC_{50} values (μM)[a] in SK-BR-3 cells at	
	Day 2	Day 4	Day 2	Day 4
1	5.6±0.3	3.4±0.3	13.4±0.7	3.5±0.2
2	50.7±1.5	21.9±1.4		
3	7.5±0.4	3.6±0.2		
4	2.1±0.1	0.9±0.1	4.6±0.2	1.0±0.1
5	47.8±2.2	29.3±1.8		
6	9.4±0.4	5.9±0.5	20.1±0.9	8.4±0.3
7	32.4±1.1	18.3±1.4		
8	68.1±3.0	24.6±1.5		
9	12.6±0.5	4.8±0.2		
10	16.4±0.5	5.3±0.2		

Concentrations of novel synthetic compounds required to inhibit by 50% (IC_{50} values) the metabolic activity of L1210 and SK-BR-3 tumor cells, using the MTS:PMS assay after 2 and 4 days of culture *in vitro*. IC_{50} values (μM) were calculated from linear regression of the slopes of the log-transformed concentration-survival curves. [a]Mean±SD (n=3).

which is absent from resting cells (G_0), is present during all active phases of the cell cycle (G_1, S, G_2) and mitosis (24). Since Ki-67 expression is strictly associated with cell proliferation, it is an excellent marker for determining the growth fraction of tumor cell populations (24). As compared to the level of Ki-67 protein detected by immunolabeling in untreated control SK-BR-3 tumor cells, the ability of 62.5-156.25 μM **4** to inhibit Ki-67 expression by 41.5-71.1% at 24 h suggests that this novel antiproliferative compound maintains surviving tumor cells in the resting stage and prevents them from re-entering the cell cycle to divide (Figure 3). After antiproliferative treatment with **4**, therefore, there are fewer tumor cells and they fail to express Ki-67. On an equimolar concentration basis, **4** inhibits Ki-67 expression more effectively than **1** and **6** but is substantially less potent than Mitox, which at 0.64-1.6 μM reduced Ki-67 protein level by 57.5-87.4% (Figure 3).

Inhibition of macromolecule syntheses. A 90-min treatment with **4** is sufficient to inhibit the incorporation of [^{3}H]thymidine into DNA used to assess the rate of DNA synthesis over a 30-min period of pulse-labeling in L1210 tumor cells *in vitro* (Figure 4). This concentration-dependent inhibition of DNA synthesis by **4** is maximal at 25 μM and characterized by an IC_{50} value of 10.1 μM (Figure 4). Under similar experimental conditions, Mitox inhibits DNA synthesis in L1210 cells with an IC_{50} value of 0.142 μM (data not shown). Besides DNA synthesis, a 3-h treatment with **4** also inhibits, in a concentration-dependent manner, the rates of RNA and protein syntheses determined over 1-h periods of pulse-labeling in L1210 tumor cells *in vitro* (Figure 5). In general, the concentrations of **4** required to inhibit RNA and protein syntheses (Figure 5) are similar to those that inhibit DNA synthesis (Figure 4): concentrations of **4** ≥10 μM have to be used to demonstrate effectiveness and maximal or near maximal inhibitions of RNA and protein syntheses are achieved at 25-62.5 μM. Under similar conditions, 62.5 μM of **4** matches the ability of a positive control of 4 μM DAU to inhibit RNA and protein syntheses by 90.5-94.4% (Figure 5).

DNA binding and fragmentation. High concentrations of antiproliferative **4** and reference anticancer drugs were evaluated for their DNA-binding affinity in a cell-free system, using the classic EB displacement assay to identify intercalating or non-intercalating drugs that destabilize the DNA double helix. Whether administered as pre- or post-treatments, 3.2-781.25 μM concentrations of **4** do not induce a loss of EB fluorescence, suggesting that this antiproliferative compound does not directly interact with double-stranded ct DNA to disrupt its structural and functional integrity and prevent the dye from intercalating into DNA base pairs (Figure 6). In contrast, positive controls of 3.2-125 μM Mitox,

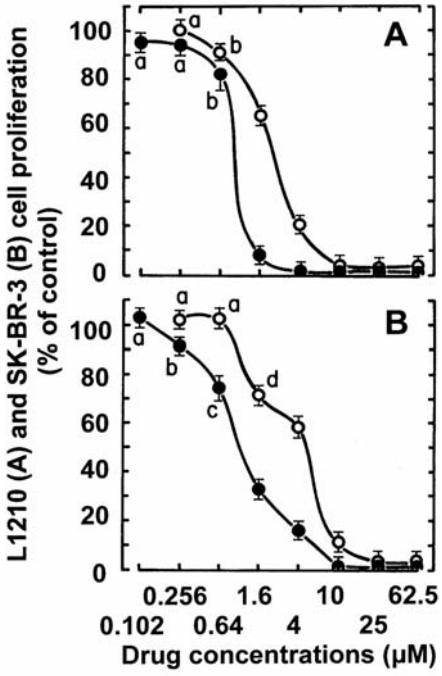

Figure 2. *Comparison of the ability of serial concentrations (plotted on a logarithmic scale) of* ***4*** *to inhibit the metabolic activity of L1210 (top panel A) and SK-BR-3 (bottom panel B) tumor cells at days 2 (○) and 4 (●) in vitro. L1210 cell proliferation results were expressed as % of the net absorbance of MTS/formazan after bioreduction by vehicle-treated control cells after 2 ($A_{490\ nm}$=1.111±0.029, 100±2.6%) and 4 ($A_{490\ nm}$=1.166±0.047, 100±4.0%) days in culture. The blank values ($A_{490\ nm}$=0.512 at day 2 and 0.508 at day 4) for cell-free culture medium supplemented with MTS:PMS reagent were subtracted from the results. For SK-BR-3 cells, the results were expressed as % of controls at days 2 ($A_{490\ nm}$=1.359±0.029, 100±2.1%) and 4 ($A_{490\ nm}$=1.235±0.040, 100±3.2%) after subtracting the blanks ($A_{490\ nm}$=0.453 at day 2 and 0.482 at day 4). Bars: means±SD (n=3).* [a]*Not different from respective controls;* [b]*p<0.025,* [c]*p<0.005 and* [d]*p<0.0005, lower than respective controls.*

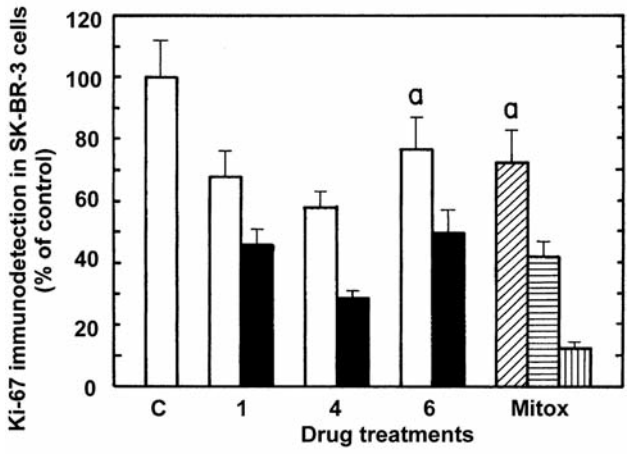

Figure 3. *Whole-cell immunodetection of Ki-67 protein level in vitro. Comparison of the abilities of 62.5 (open columns) and 156.25 μM (solid columns) concentrations of* ***1****,* ***4*** *and* ***6*** *to inhibit the Ki-67 marker of cell proliferation in SK-BR-3 cells at 24 h. The magnitude of Ki-67 inhibition caused by 0.256 (diagonal stripes), 0.64 (horizontal stripes) and 1.6 μM (vertical stripes) mitoxantrone (Mitox) was used as positive control. The results were expressed as % of the ratio of Ki-67 protein level (relative luminescence intensity of the anti-Ki-67 primary antibody-antigen immune complex bound to horseradish peroxidase-linked secondary antibody):cell number (relative fluorescence intensity of the Hoechst reagent-DNA complex) in vehicle-treated control SK-BR-3 tumor cells at 24 h (C: 1.8110±0.2137, 100±11.8%). Bars: means±SD (n=3).* [a]*p<0.05, smaller than control.*

actinomycin D (Act-D) and amsacrine (*m*-AMSA; 4'-[9-acridinylamino]methanesulfon-*m*-anisidide), which destabilize double-stranded ct DNA to prevent or disrupt EB intercalation, almost totally suppress the fluorescence of the EB-DNA complex (inhibition by 61.4-95.9%) (Figure 6). Under these experimental conditions, the concentration-dependent inhibitions of EB binding to DNA by Mitox, Act-D and *m*-Amsa have IC_{50} values of 1.2, 3.4 and 31.0 μM, respectively (data not shown). The ability of compound **4** to induce DNA fragmentation at 24 h was assessed and compared to those of DAU and Mitox, using L1210 cells containing ^{3}H-thymidine-prelabeled DNA to detect low molecular weight DNA fragments after intact chromatin precipitation (Figure 7). As compared to untreated controls (2.8% DNA fragmentation), the concentration-dependent induction of DNA cleavage caused by **4** in L1210 cells at 24 h started at 4 μM and peaked at 156.25 μM (22.2% DNA fragmentation) before declining towards control values at the highest 390.625 μM concentration tested (Figure 7). The fact that 1.6 μM DAU matched the 2.6-fold stimulation of DNA fragmentation caused by 10 μM **4** and that 0.256 μM Mitox surpasses the 4.0-fold stimulation of DNA fragmentation caused by 25 μM **4** suggests that antiproliferative compound **4** is 6-98 times less cytotoxic than the above anticancer drugs.

Mitotic index and abnormalities. Control populations of L1210 tumor cells cultured for 12-48 h in the absence of drugs contain only 0.46% of mitotic cells, 2.24% of binucleated cells (Figure 8), 0.23% of multinucleated cells, and have no micronuclei (Figure 9). In relation to their ability to disrupt microtubule dynamics, treatments for 12-48 h with vincristine (VCR), which blocks tubulin polymerization and microtubule assembly, and taxol, which lowers the critical concentration of free tubulin required to promote polymerization and blocks microtubule disassembly, respectively produce 15.7- to 64.2- and 7.7- to 20.4-fold increases in the mitotic index (Figure 8A). Such microtubule de-stabilizing and stabilizing anticancer drugs known to block cell cycle progression in M-phase, therefore, served as positive controls in this antimitotic assay. Under similar

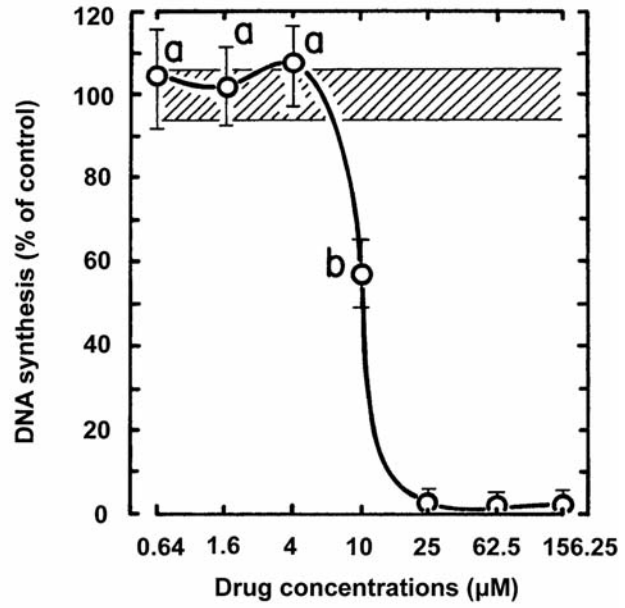

Figure 4. *Comparison of the ability of serial concentrations (logarithmic scale) of **4** to inhibit the rate of incorporation of [^{3}H]thymidine into DNA measured in L1210 cells over 30 min following a 90-min period of incubation at 37˚C in vitro. DNA synthesis in vehicle-treated control cells at 37˚C was 13,797±814 cpm (100±5.9%, striped area). The blank value (1,189±73 cpm) for control cells incubated and pulse-labeled at 2˚C with 1 μCi of [^{3}H]thymidine has been subtracted from the results. Bars: means±SD (n=3). [a]Not different from control; [b]p<0.005, less than control.*

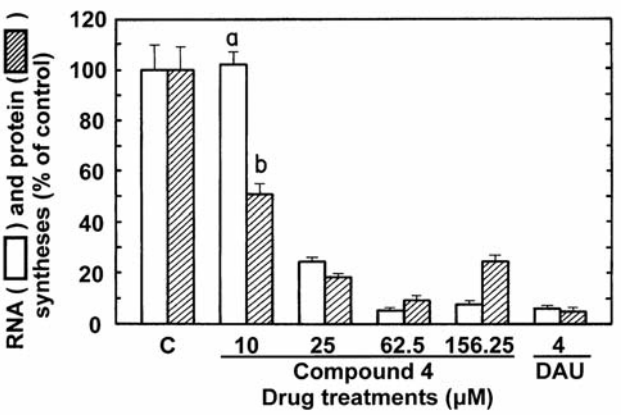

Figure 5. *Comparison of the ability of 10, 25, 62.5 and 156.25 μM concentrations of **4** to inhibit the rates of incorporation of [^{3}H]uridine into RNA (open columns) and [^{3}H]leucine into protein (striped columns) measured in L1210 cells over 1 h following a 3-h period of incubation at 37˚C in vitro. The magnitudes of RNA and protein synthesis inhibition caused by 4 μM daunorubicin (DAU) were used as positive controls. In vehicle-treated control cells (C) at 37˚C, RNA synthesis was 28,057±2,609 cpm (100±9.3%) and protein synthesis was 7,324±637 cpm (100±8.7%). The blank values for control cells incubated and pulse-labeled at 2˚C with 2 μCi of [^{3}H]uridine (6,305±719 cpm) or 2.5 μCi of [^{3}H]leucine (4,032±375 cpm) have been subtracted from the results. Bars: means±SD (n=3). [a]Not different from control; [b]p<0.005, less than control.*

conditions, antiproliferative concentrations of compound **4** 12.8 to 80 times greater than those of VCR and taxol produce weak 1.4- to 5.1-fold increases in the mitotic index of L1210 tumor cells at 12-48 h (Figure 8A) but nearly match the abilities of VCR and taxol to stimulate the formation of binucleated (2.1- to 5.7-fold increases in Figure 8B) and multinucleated cells (2.4- to 21.0-fold increases in Figure 9A), and produce a substantial 0.1-1.5% of cells with micronuclei (Figure 9B), suggesting that this compound might enhance mitotic abnormality, induce chromosomal damage or missegregation, and block cytokinesis. In the same experiments, microtubule de-stabilizing VCR is ineffective at 12-24 h and needs 48 h to raise the percentage of binucleated (2.7-fold increase in Figure 8B) and multinucleated cells (16.1-fold increase in Figure 9A) above the background level observed in untreated control cells, and to produce 0.5% of cells with micronuclei (Figure 9B), whereas microtubule-stabilizing taxol produces time-dependent increases in the incidence of cells containing 2 nuclei (2.2- to 7.0-fold stimulation in Figure 8B) and 3-4 nuclei (4.2- to 30.6-fold stimulation in Figure 9A), and induces a 5.6% of cells with micronuclei (Figure 9B). This is in agreement with the fact that taxol-treated cells with stabilized spindle microtubules escape from mitosis without cytokinesis and proceed as binucleated cells to the next round of DNA synthesis to form polynucleated polyploid cells which eventually die (28).

Discussion

The 2-halo-3-aryl-4(3*H*)-quinazoliniminium halides **1-10** were synthesized by an intramolecular cyclization of benzannulated cyano-ene-carbodiimides in the presence of a hydrogen halide generated *in situ*. Among all quinazoliniminium halides synthesized, the 2-chloro-3-(4-methoxyphenyl)quinazolin-4(3*H*)-iminium chloride **4** is consistently the most effective against L1210 tumor cell proliferation, suggesting that the presence of a para methoxyphenyl substituent on the N3 of **4** enhances the antiproliferative properties of the quinazoliniminium scaffold. The excellent hydrogen bond accepting properties of the oxygen atom of the methoxy group may contribute to a tighter binding of **4** to its yet undetermined biological target(s). A methoxy group may also enhance the antioxidant properties of the compound because of its electron donating nature.

However, the quinazoliniminium halides **1-3** and **5-10** were unable to match or surpass the antiproliferative effect of **4** in L1210 cells. The chloride and iodide salts of 2-chloro-3-phenyl-4(3*H*)-quinazoliniminiums **1** and **3**, respectively, have

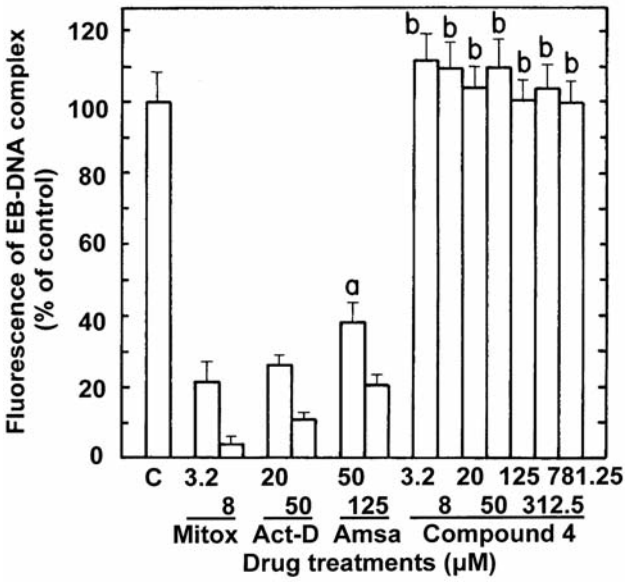

Figure 6. *Comparison of the ability of serial concentrations of mitoxantrone (Mitox), actinomycin D (Act-D), m-amsacrine (Amsa) and* ***4*** *to inhibit the binding of EB to double-stranded ct DNA. Results were expressed as % of the control (C) fluorescence of the EB-DNA complex in the absence of drug at 525 nm excitation and 600 nm emission (153.6±12.7 arbitrary units; 100±8.3%). The background of EB fluorescence in the absence of DNA (26.4±1.9 arbitrary units) was subtracted from the results. Bars: means±SD (n=3).* [a]*p<0.0005, smaller than control;* [b]*Not different from control.*

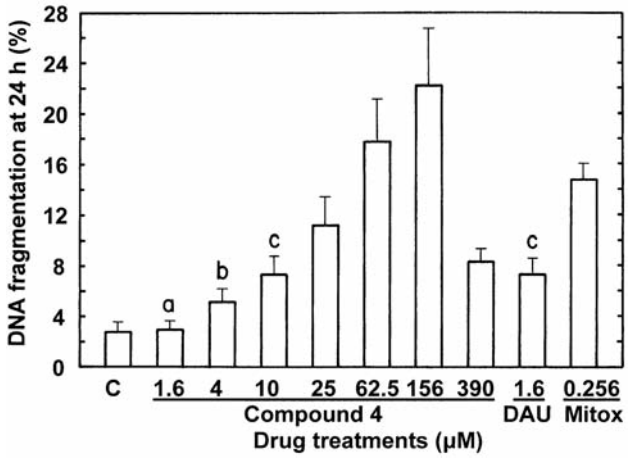

Figure 7. *Comparison of the ability of 1.6, 4, 10, 25, 62.5, 156.25 and 390.625 μM concentrations of* ***4*** *to induce DNA fragmentation at 24 h in L1210 cells containing* ^{3}*H-prelabeled DNA in vitro. The levels of DNA fragmentation caused by 1.6 μM daunorubicin (DAU) and 0.256 μM mitoxantrone (Mitox) were used as positive controls. The results were expressed as [cpm in supernatant/(cpm in supernatant + pellet)] ×100 at 24 h. For vehicle-treated control (C) tumor cells (2.79±0.76% DNA fragmentation), the supernatant (DNA fragments) was 1,651±453 cpm and the pellet (intact DNA) was 57,513±15,552 cpm. Bars: means±SD (n=3).* [a]*Not different from control;* [b]*p<0.025 and* [c]*p<0.01, greater than control.*

equipotent antiproliferative activity but the corresponding bromide salt **2** is 6-8 times less potent than **1** and **3** against L1210 cell proliferation at 2-4 days, suggesting that a bromide counter ion decreases the bioactivity of the quinazoliniminium scaffold. It would be interesting to determine if the methoxy substituent that boosts the antiproliferative activity of the 2-chloro-3-(4-methoxyphenyl) quinazolin-4(3*H*)-iminium chloride **4** would similarly enhance the bioactivity of the corresponding iodide salt. The replacement of the methoxy group on the phenyl ring of 4 by an ethyl ester functionality or a chlorine atom in **5** and **6**, respectively, decreases the antiproliferative activities by 23-33 and 5-7 times. The decrease in activity is more drastic in the case of **5** as compared to **6** which may be due to the larger size of the ethyl ester functionality as opposed to a chlorine atom leading to inefficient binding in the active site of the target(s). Changing the position of the chlorine atom from *para* to *meta* or *ortho* on the phenyl ring further inhibits the bioactivity since compounds **7** and **8** are, respectively, 3 and 4-7 times less effective than **6** against L1210 cell proliferation. Finally, compounds **9** and **10** are both less effective than **1**, suggesting that methylations on the second aromatic ring are equally disruptive for the antiproliferative activity of the quinazoliniminium chlorides.

The most potent compound **4** and two other derivatives **1** and **6** were also investigated for antiproliferative activity against SK-BR-3 tumor cells. The fact that the IC_{50} values of **1**, **4** and **6** required to inhibit the mitochondrial ability of tumor cells to metabolize the MTS:PMS reagent at days 2 and 4 are slightly higher in SK-BR-3 than L1210 cells suggests that the antiproliferative action of quinazoliniminium salts is generally greater against unsynchronized populations of rapidly-growing suspensions of leukemia cells that are frequently turning through the cell cycle than against unsynchronized populations of relatively slow-growing adherent monolayers of solid tumor cells that have smaller growth fractions. In addition, because **4**, **4** and **6** are not more effective in SK-BR-3 cells than in L1210 cells, these antiproliferative compounds are unlikely to specifically target the ligand-dependent human epidermal growth factor receptor-2 (HER2) signaling pathway linked to the proliferation of these HER2-overexpressing human breast cancer cells. Such lack of improvement for the antiproliferative potency of **1**, **4** and **6** between L1210 and HER2-overexpressing tumor cells suggests that the antitumor activity of these compounds is not affected by the growth receptor dependency of the neoplastic cells. Since the concentration-dependent inhibitions of L1210 and SK-BR-3 tumor cell proliferation by **4** are more pronounced at 4 than 2 days, the effectiveness of this bioactive compound is clearly a combination of drug concentration and duration of action. Based on their ability to inhibit both

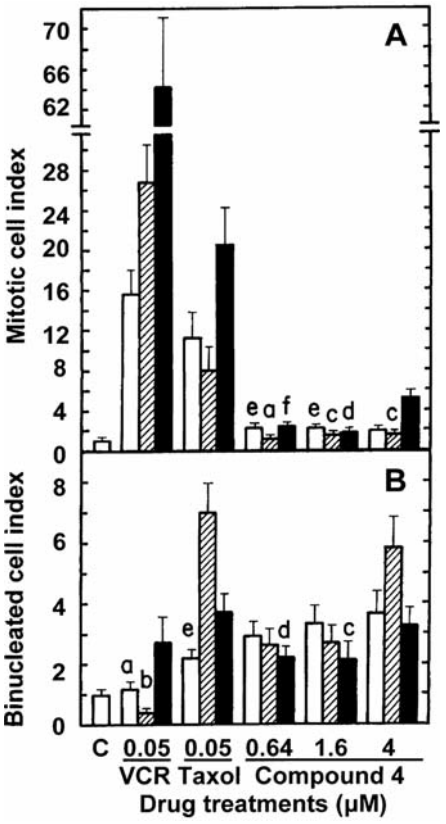

Figure 8. *Comparison of the effects of **4**, vincristine (VCR) and taxol on the frequency of mitotic figures (A) and binucleated cells (B) in L1210 tumor cells in vitro. L1210 cells were incubated in triplicate for 12 (open columns), 24 (striped columns) and 48 h (closed columns) at 37˚C in the presence or absence (C: control) of the indicated concentrations of drugs. The percentage of cells in each category was determined by morphologic analysis, scoring at least 2,000 cells/slide to identify those containing mitotic figures or 2 nuclei. Results were expressed as % of mitotic (A) or binucleated cells (B) in drug-treated cultures divided by the % of mitotic (C: 0.46±0.11%) or binucleated cells (C: 2.24±0.56%) in vehicle-treated controls. Bars: means±SD (n=3). [a]Not different from respective controls; [b]p<0.025, less than control; [c]p<0.05, [d]p<0.025, [e]p<0.01, and [f]p<0.005, greater than respective controls.*

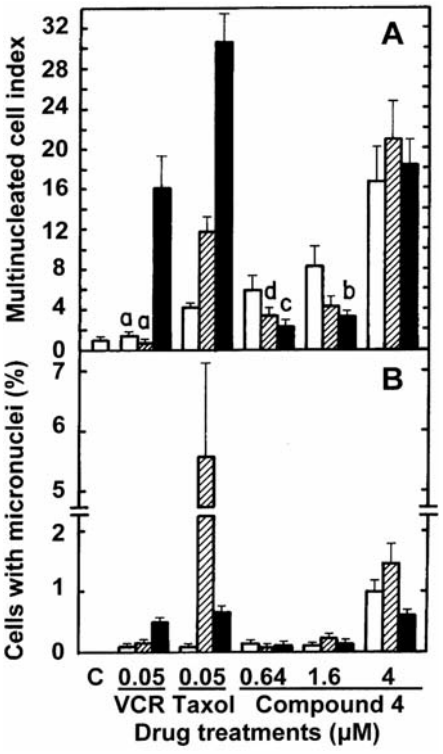

Figure 9. *Comparison of the effects of **4**, vincristine (VCR) and taxol on the frequencies of multinucleated cells (A) and micronuclei (B) in L1210 tumor cells in vitro. L1210 cells were incubated in triplicate for 12 (open columns), 24 (striped columns) or 48 h (closed columns) at 37˚C in the presence or absence (C: control) of the indicated concentrations of drugs. The percentage of cells in each category was determined by morphologic analysis, scoring at least 2,000 cells/slide to identify those containing 3-4 nuclei or micronuclei. A: Results were expressed as % of multinucleated cells in drug-treated cultures divided by the % of multinucleated cells in vehicle-treated controls (C: 0.23±0.05%). B: Results were expressed as % of drug-treated cells with micronuclei (C: 0%). Bars: means±SD (n=3). [a]Not different from respective controls; [b]p<0.05, [c]p<0.025, and [d]p<0.005, greater than control.*

leukemic and mammary tumor cell proliferation, these quinazoliniminium halides might also be effective across a wide spectrum of tumor cell lines.

The Ki-67 protein, which is absent from resting cells (G_0), can be exclusively detected within the nuclei of cells progressing through the G_1, S and G_2 phases of the cell cycle and relocates to the surface of the chromosomes during mitosis (24). Because Ki-67 expression may be absolutely required to maintain tumor cell proliferation, the fraction of Ki-67-positive tumor cells is often correlated with the clinical course of cancer (24). Hence, it is significant to show that micromolar concentrations of **4** can substantially inhibit the expression of Ki-67 antigen for at least 24 h in human SK-BR-3 cells, suggesting that this novel antitumor compound might be effective for reducing the growth fraction of tumor cell populations and controlling disease progression. Although it may be somewhat misleading to compare biological responses measured at very different times, the concentration-dependent inhibitions of DNA, RNA and protein syntheses by **4** suggest that the ability of this compound to prevent tumor cells from synthesizing macromolecules at 2-3 h (Figures 4 and 5) may play a role in its inhibition of Ki-67 expression at 24 h (Figure 3) and antiproliferative activity at days 2 and 4 (Table I and Figure 2). In accord with the effects of established anticancer drugs used as positive controls, concentrations of **4** higher than those sufficient to inhibit tumor cell proliferation must be used to inhibit Ki-67 expression and DNA, RNA and protein

syntheses or maximally induce DNA fragmentation. Such apparent discrepancy may simply be due to different experimental conditions and cellular responses to various periods of drug exposure: the rate of macromolecule syntheses over 0.5-1 h are inhibited in cells treated for only 2-3 h with **4** or DAU, the level of Ki-67 protein is reduced in cells incubated for 24 h in the presence of **4** or Mitox, and DNA fragmentation occurs 24 h after treatment with such antitumor compounds, whereas the more spectacular inhibitions of L1210 and SK-BR-3 tumor cell proliferations are the result of 2- and 4-day long drug treatments.

FDA-approved Mitox is a synthetic anthracenedione related to DAU but which is less cardiotoxic. Besides targeting the DNA topoisomerase II enzyme to induce DNA damage, the mechanism of action of anthracycline-type antitumor drugs involves intercalation of the planar aglycone moiety into DNA to disrupt DNA replication and transcription (29). The 9-anilinoacridine drug *m*-Amsa is known to quench EB-DNA fluorescence and its anti-leukemic activity requires intercalative DNA binding (30, 31). Although alternative binding modes that include single-stranded DNA have also been proposed, the antitumor antibiotic Act-D blocks RNA polymerase and transcription by binding to double-stranded DNA. Act-D complexes with duplex DNA by intercalation of its planar aromatic rings between adjacent base pairs of the double helix, the dinucleotide site GpC exhibiting an especially high binding affinity for Act-D (32). In addition, *m*-Amsa preferentially targets and inhibits DNA topoisomerase II activity, whereas Act-D is likely a dual inhibitor of DNA topoisomerase I and II enzymes (33-35). Hence, the present EB results are consistent with the fact that Mitox (3.2-8 μM), Act-D (20-50 μM) and *m*-Amsa (50-125 μM) are DNA-reactive agents that intercalate into DNA and cause crosslinks and strand breaks. However, the observation that even higher concentrations of **4** up to 781.25 μM do not directly bind to purified DNA to inhibit the fluorescence of the EB-DNA complex in a cell-free assay, suggests that quinazoliniminium salts are unlikely to directly target cellular DNA to exert their antitumor activities.

In contrast to the early cleavage of DNA into large 50-300 kbp fragments, an initial signaling event that may induce tumor cells treated with relatively low concentrations of DNA-damaging anticancer drugs to commit apoptosis, the secondary endonucleolytic degradation of DNA at internucleosomal linker sites to produce small 180-200 bp mono- and oligonucleosomal fragments at 24 h is a late marker concurrent with morphological evidence of apoptosis (36). Antiproliferative concentrations of **4** induce DNA fragmentation in L1210 cells at 24 h, suggesting that the ability of quinazoliniminium salts to trigger apoptotis may play a significant role in their molecular mechanism of action. Since apoptosis is an active ATP-driven and cell cycle phase-specific process that requires the expression of specific genes, the synthesis of new RNA and proteins, and the activation of caspases, non-caspase proteases and nucleases, inhibition of such mechanisms can prevent apoptotic DNA fragmentation (37). Hence, the fact that the concentration-dependent induction of DNA fragmentation by **4** in L1210 cells at 24 h is characterized by a biphasic response, increasing at 4-62.5 μM with a peak at 156 μM and then decreasing at 390 μM, suggests that, even though they are increasingly cytostatic, the highest concentrations of antiproliferative quinazoliniminium salts may inhibit DNA and other macromolecule syntheses to such excessive degrees and become so cytotoxic as to abolish their own ability to sustain the active process of apoptosis and internucleosomal DNA fragmentation induced by the lower concentrations of these compounds (37). Even though **4** does not directly bind to DNA, the abilities of this antitumor compound to interact with maintenance enzymes or regulatory proteins and indirectly cause high molecular weight DNA-strand breaks, crosslinks or chromosome aberrations and cytokinesis disruption remain to be determined. Therefore, it is rather premature to speculate on the nature of the primary molecular targets, massive damaging events and nuclear signals that induce **4**-treated tumor cells to undergo mitotic disruption and apoptotic DNA degradation.

Despite the 5.1-fold increase in the number of L1210 cells treated with 4 μM of **4** that display mitotic figures at 48 h, the inability of **4** to dramatically raise the mitotic index of L1210 cells like VCR and taxol do at 12-48 h suggests that this compound is not a valuable mitotic spindle poison and is unlikely to specifically target tubulin and alter the polymerization/depolymerization of microtubules in order to elicit its antiproliferative activity. But increasingly antiproliferative concentrations of **4** (0.64-4 μM) might trigger some genotoxic effects to substantially increase the levels of binucleated cells, multinucleated cells and micronuclei in L1210 tumor cells at 12-48 h. Binucleated cells indicate that cytokinesis is inhibited following nuclear division (27). Multinucleated cells may follow if binucleated cells re-enter the cell cycle and escape further cytokinesis. The micronucleus test is an indicator of drug-induced chromosomal damage and aberration as such structures generally form during the metaphase/anaphase transition of mitosis when a whole lagging chromosome or an acentric chromosome fragment resulting from a clastogenic or mutagenic event fail to integrate into the daughter nuclei (27). However, chromosome aberration and non-disjunction/ missegregation might be the consequence of prolonged drug-induced mitotic disruption and might be responsible for cellular inability to undergo cytokinesis after regression of the cleavage furrow (38). If completion of cytokinesis requires accurate chromosome segregation, it is possible that **4** treatment induces chromosome aberration and missegregation to increase the frequency of binucleated cells, multinucleated cells and micronuclei. The results are encouraging given the fact that the interesting antitumor

activity of compound **4** was discovered among only a handful of quinazoliniminium salts synthesized and opens the possibility of designing new anticancer drugs based on this framework. Further structure–activity studies are required to identify more potent antitumor lead compounds and characterize their molecular targets and mechanisms of action.

Acknowledgements

This study was supported in part by grants from Kansas State University (Innovative Research Award from the Terry C. Johnson Center for Basic Cancer Research and Research Seed Grant Award from the Biology Research and Instruction Enhancement Fund Program).

References

1 Horton DA, Bourne GT and Smythe ML: The combinatorial synthesis of bicyclic privileged structures or privileged substructures. Chem Rev (Washington, DC, U.S.) *103*: 893-930, 2003.

2 Hess HJ, Cronin TH and Scriabine A: Antihypertensive 2-amino-4(3H)-quinazolinones. J Med Chem *11*: 130-136, 1968.

3 Chen Z, Hu G, Li D, Chen J, Li Y, Zhou H and Xie Y: Synthesis and vasodilator effects of rutaecarpine analogues which might be involved transient receptor potential vanilloid subfamily, member 1 (TRPV1). Bioorg Med Chem *17*: 2351-2359, 2009.

4 Kubota H, Kakefuda A, Watanabe T, Ishii N, Wada K, Masuda N, Sakamoto D and Tsukamoto S-I: Synthesis and pharmacological evaluation of 1-oxo-2-(3-piperidyl)-1,2,3,4-tetrahydroisoquinolines and related analogues as a new class of specific bradycardic agents possessing I(f) channel inhibitory activity. J Med Chem *46*: 4728-4740, 2003.

5 Hirai S, Kikuchi H, Kim H-S, Begum K, Wataya Y, Tasaka H, Miyazawa Y, Yamamoto K and Oshima Y: Metabolites of febrifugine and its synthetic analogue by mouse liver S9 and their antimalarial activity against *Plasmodium malaria* parasite. J Med Chem *46*: 4351-4359, 2003.

6 Gudasi KB, Shenoy RV, Vadavi RS, Patil MS and Patil SA: New lanthanide (III) complexes of biologically active 2,3-disubstituted quinazoline-4-(3*H*)-one: synthesis, characterization and biological studies. Indian J Chem (Sect A: Inorg Bio-inorg, Phys, Theor Anal Chem) *44A*: 2247- 2254, 2005.

7 Alagarsamy V: Antibacterial and antifungal activities of some novel 2,3-disubstituted quinazolin-4(3*H*)-ones. Indian J Pharm Sci *64*: 600-603, 2002.

8 Reddy PB, Reddy SM, Reddy KL and Lingaiah P: Laboratory evaluation of antimicrobial activity of 2,3-disubstituted quinazoline (3H) 4-ones and their metal complexes. Indian Phytopathol *38*: 361-364, 1985.

9 Rudolph J, Esler WP, O'Connor S, Coish PDG, Wickens PL, Brands M, Bierer DE, Bloomquist BT, Bondar G, Chen L, Chuang C-Y, Claus TH, Fathi Z, Fu W, Khire UR, Kristie JA, Liu X-G, Lowe DB, McClure AC, Michels M, Ortiz AA, Ramsden PD, Schoenleber RW, Shelekhin TE, Vakalopoulos A, Tang W, Wang L, Yi L, Gardell SJ, Livingston JN, Sweet LJ and Bullock WH: Quinazolinone derivatives as orally available ghrelin receptor antagonists for the treatment of diabetes and obesity. J Med Chem *50*: 5202-5216, 2007.

10 Jatav V, Mishra P, Kashaw S and Stables JP: CNS depressant and anticonvulsant activities of some novel 3-[5-substituted 1,3,4-thiadiazole-2-y1]-2-styryl quinazoline-4(3H)-ones. Eur J Med Chem *43*: 1945-1954, 2008.

11 Al-Obaid AM, Abdel-Hamide SG, El-Kashef HA, Abdel-Aziz AAM, El-Azab AS, Al-Khamees HA and El-Subbagh HI: Substituted quinazolines, part 3. Synthesis, *in vitro* antitumor activity and molecular modeling study of certain 2-thieno-4(3*H*)-quinazolinone analogs. Eur J Med Chem *44*: 2379-2391, 2009.

12 Giri RS, Thaker HM, Giordano T, Williams J, Rogers D, Sudersanam V and Vasu KK: Design, synthesis and characterization of novel 2-(2,4-disubstituted-thiazole-5-yl)-3-aryl-3H-quinazolin-4-one derivatives as inhibitors of NF-κB and AP-1 mediated transcription activation and as potential anti-inflammatory agents. Eur J Med Chem *44*: 4783, 2009.

13 Chandrika PM, Yakaiah T, Rao ARR, Narsaiah B, Reddy NC, Sridhar V and Rao JV: Synthesis of novel 4,6-disubstituted quinazoline derivatives, their anti-inflammatory and anticancer activity (cytotoxic) against U937 leukemia cell lines. Eur J Med Chem *43*: 846-852, 2008.

14 Kumar A, Sharma S, Archana, Bajaj K, Sharma S, Panwar H, Singh T and Srivastava VK: Some new 2,3,6-trisubstituted quinazolinones as potent anti-inflammatory, analgesic and COX-II inhibitors. Bioorg Med Chem *11*: 5293-5299, 2003.

15 Sindrup SH, Graf A and Sfikas N: The NK1-receptor antagonist TKA731 in painful diabetic neuropathy: a randomized, controlled trial. Eur J Pain (Amsterdam, Neth) *10*: 567-571, 2006.

16 Patel SV, Patel MP and Patel RG: Synthesis and characterization of heterocyclic substituted fluoran compounds. J Serb Chem Soc *72*: 1039-1044, 2007.

17 Patel VH, Patel MP and Patel RG: Disperse dyes based on 2-methyl-3-[3'-aminophthalimido]-4(3*H*)-quinazolinone. J Serb Chem Soc *67*: 719-726, 2002.

18 Luo H-Y, Zhang X-B, He C-L, Shen G-L and Yu R-Q: Synthesis of dipicolylamino substituted quinazoline as chemosensor for cobalt (II) recognition based on excited-state intramolecular proton transfer. Spectrochim Acta (Part A: Mol Biomol Spectroscopy) *70A*: 337-342, 2008.

19 Jaen JC, Gregor VE, Lee C, Davis R and Emmerling M: Acetylcholinesterase inhibition by fused dihydroquinazoline compounds. Bioorg Med Chem Lett *6*: 737-742, 1996.

20 Decker M, Kraus B and Heilmann J: Design, synthesis and pharmacological evaluation of hybrid molecules out of quinazolinimines and lipoic acid lead to highly potent and selective butyrylcholinesterase inhibitors with antioxidant properties. Bioorg Med Chem *16*: 4252-4261, 2008.

21 Decker M: Homobivalent quinazolinimines as novel nanomolar inhibitors of cholinesterases with dirigible selectivity toward butyrylcholinesterase. J Med Chem *49*: 5411-5413, 2006.

22 Decker M, Krauth F and Lehmann J: Novel tricyclic quinazolinimines and related tetracyclic nitrogen bridgehead compounds as cholinesterase inhibitors with selectivity towards butyrylcholinesterase. Bioorg Med Chem *14*: 1966-1977, 2006.

23 Perchellet EM, Crow KR, Gakhar G, Nguyen TA, Shi A, Hua DH and Perchellet J-P: Bioactivity and molecular targets of novel substituted quinolines in murine and human tumor cell lines *in vitro*. Int J Oncology *36*: 673-688, 2010.

24 Scholzen T and Gerdes J: The Ki-67 protein: from the known and the unknown. J Cell Physiol *182*: 311-322, 2000.

25 Cory AH, Owen JC, Barltrop JA and Cory JG: Use of an aqueous soluble tetrazolium/formazan assay for cell growth assays in culture. Cancer Commun *3*: 207-212, 1991.
26 Morgan AR, Lee JS, Pulleyblank DS, Murray NL and Evans DH: Ethidium fluorescence assays. Part 1. Physico-chemical studies. Nucleic Acids Res *7*: 547-569, 1979.
27 Fenech M, Chang WP, Kirsch-Volders M, Holland N, Bonassi S and E. Zeiger E: HUMN project: detailed description of the scoring criteria for the cytokinesis-block micronucleus assay using isolated human lymphocyte cultures. Mutat Res *534*: 65-75, 2003.
28 Lieu C-H, Chang Y-N and Lai Y-K: Dual cytotoxic mechanisms of submicromolar taxol on human leukemia HL-60 cells. Biochem Pharmacol *53*: 1587-1596, 1997.
29 Gewirtz DA: A critical evaluation of the mechanisms of action proposed for the antitumor effects of the anthracycline antibiotics adriamycin and daunorubicin. Biochem Pharmacol *57*: 727-741, 1999.
30 Baguley BC and Le Bret M: Quenching of DNA-ethidium fluorescence by amsacrine and other antitumor agents: a possible electron-transfer effect. Biochemistry *23*: 937-943, 1984.
31 Denny WA, Twigden SJ and Baguley BC: Steric constraints for DNA binding and biological activity in the amsacrine series. Anticancer Drug Des *1*: 125-132, 1986.
32 Snyder JG, Hartman NG, Langlois D'Estantoit B, Kennard O, Remeta DP and Breslauer KJ: Binding of actinomycin D to DNA: evidence for a nonclassical high-affinity binding mode that does not require GpC sites. Proc Natl Acad Sci USA *86*: 3968-3972, 1989.
33 Nelson EM, Tewey KM and Liu LF: Mechanism of antitumor drug action: poisoning of mammalian DNA topoisomerase II on DNA by 4'-(9-acridinylamino)-methanesulfon-*m*-anisidide. Proc Natl Acad Sci USA *81*: 1361-1365, 1984.
34 Wu MH and Yung BY: Cell cycle phase-dependent cytotoxicity of actinomycin D in HeLa cells. Eur J Pharmacol *270*: 203-212, 1994.
35 Insaf SS, Danks MK and Witiak DT: A structure–function analysis of DNA topoisomerase II inhibitors. Curr Med Chem *3*: 437-466, 1996.
36 Nagata S: Apoptotic DNA fragmentation. Exp Cell Res *256*: 12-18, 2000.
37 Perchellet EM, Ward MM, Skaltsounis A-L, Kostakis IK, Pouli N, Marakos P and Perchellet J-P: Antiproliferative and proapoptotic activities of pyranoxanthenones, pyranothioxanthenones and their pyrazole-fused derivatives in HL-60 cells. Anticancer Res *26*: 2791-2804, 2006.
38 Shi Q and King RW: Chromosome nondisjunction yields tetraploid rather than aneuploid cells in human cell lines. Nature *437*: 1038-1042, 2005.

Received May 16, 2011
Revised May 27, 2011
Accepted May 31, 2011